Solar Orbiter and stereoscopic magnetometry

Andreas Lagg

Max-Planck-Institut für Sonnensystemforschung
Katlenburg-Lindau, Germany

1st SOLARNET meeting, Oslo, Aug 6 2013

Table of Contents

Orbit

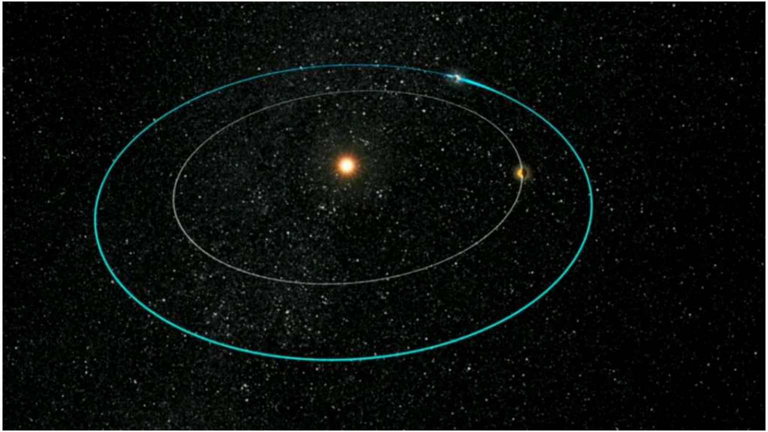

January 2017 mission profile

- Launch:
  Jan 2017
- First science perihel:
  Jul 2020 (0.28 AU)
- max. latitude:
  Jul 2025 (34°)

Remote sensing instruments

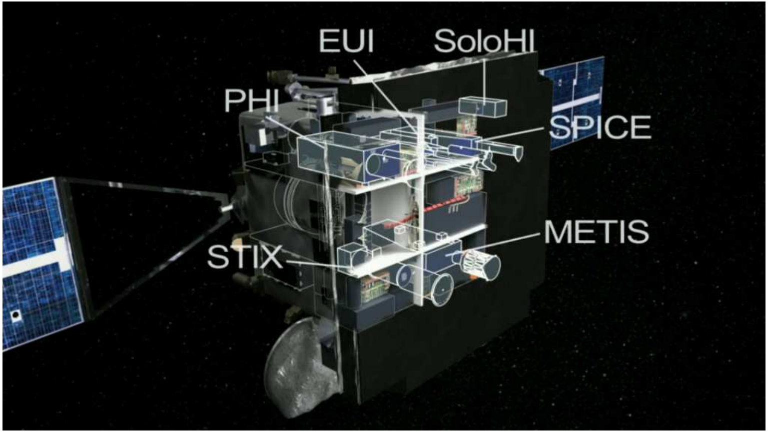

EUI Extreme Ultraviolet Imager
images of solar atmospheric layers above the photosphere

SoloHI Heliospheric Imager
quasi-steady flow and transient disturbances in the solar wind

SPICE Spectr. Imag. of the Cor. Env.
EUV spectroscopy to characterize on-disk coronal plasma

METIS Coronagraph
VIS, UV, E-UV emission (1.4 to 4.1 R_S)

STIX X-ray Spectrometer
thermal and non-thermal X-ray emission to characterize acc. electrons and high temp. thermal plasmas (flares)

PHI Polarimetric and Helioseismic Im.
. . . this talk

In-situ instruments

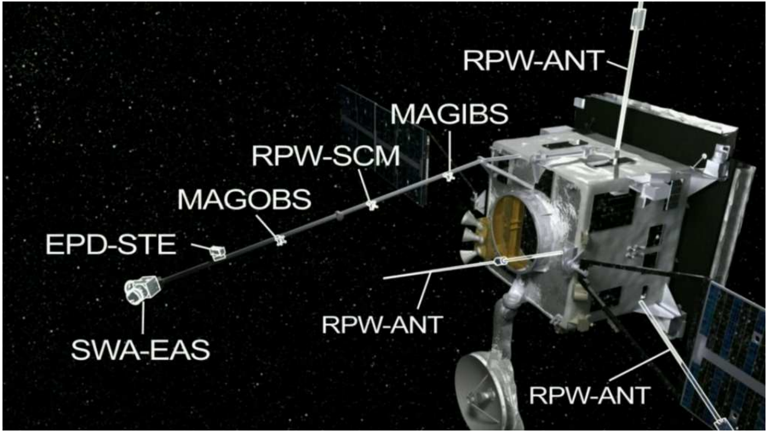

EPD Energetic Particle Detector
composition, timing and distribution functions of suprathermal and energetic particles

SWA Solar Wind Plasma Analyzer
ion and electron bulk properties (including, density, velocity, and temperature) of the solar wind

RPW Radio and Plasma Waves
magnetic and electric fields to determine the characteristics of electromagnetic and electrostatic waves in the solar wind

MAG Magnetometer
linkage of solar magnetic field into space

Polarimetric and Helioseismic Imager (SO/PHI)

SO/PHI science

Goal

SO/PHI is central to reach 3 of the 4 top level science goals. Main question: How does the solar dynamo work and drive connections between the Sun and the heliosphere?

Scope

SO/PHI probes the solar interior and provides the magnetic field at the solar surface that drives transient and energetic phenomena in the solar atmosphere and the heliosphere.

Tools

Polarimetry and local helioseismology in Fe I 6173 Å

Polarimetric and Helioseismic Imager (SO/PHI)

SO/PHI science

Goal

SO/PHI is central to reach 3 of the 4 top level science goals.
Main question: How does the solar dynamo work and drive connections between the Sun and the heliosphere?

Scope

SO/PHI probes the solar interior and provides the magnetic field at the solar surface that drives transient and energetic phenomena in the solar atmosphere and the heliosphere.

Tools

Polarimetry and local helioseismology in Fe I 6173 Å

Polarimetric and Helioseismic Imager (SO/PHI)

SO/PHI science

Goal

SO/PHI is central to reach 3 of the 4 top level science goals.
Main question: How does the solar dynamo work and drive connections between the Sun and the heliosphere?

Scope

SO/PHI probes the solar interior and provides the magnetic field at the solar surface that drives transient and energetic phenomena in the solar atmosphere and the heliosphere.

Tools

Polarimetry and local helioseismology in Fe I 6173 Å

SO/PHI - science

SO/PHI will provide unique science

- Provide B to EUV imager and spectrometer, all observing at high spatial resolution (up to 180 km): linkage science
- First decent view of magnetic and velocity field at poles
- Follow surface and subsurface evolution of solar features (e.g. active regions) without changing viewing angle
- Stereoscopic helioseismology to better probe the interior
- Stereoscopy of the photosphere

SO/PHI - science

SO/PHI will provide unique science

- Provide B to EUV imager and spectrometer, all observing at high spatial resolution (up to 180 km): linkage science
- First decent view of magnetic and velocity field at poles
- Follow surface and subsurface evolution of solar features (e.g. active regions) without changing viewing angle
- Stereoscopic helioseismology to better probe the interior
- Stereoscopy of the photosphere

SO/PHI - science

SO/PHI will provide unique science

- Provide B to EUV imager and spectrometer, all observing at high spatial resolution (up to 180 km): linkage science
- First decent view of magnetic and velocity field at poles
- Follow surface and subsurface evolution of solar features (e.g. active regions) without changing viewing angle
- Stereoscopic helioseismology to better probe the interior
- Stereoscopy of the photosphere

SO/PHI - science

SO/PHI will provide unique science

- Provide B to EUV imager and spectrometer, all observing at high spatial resolution (up to 180 km): linkage science
- First decent view of magnetic and velocity field at poles
- Follow surface and subsurface evolution of solar features (e.g. active regions) without changing viewing angle
- Stereoscopic helioseismology to better probe the interior
- Stereoscopy of the photosphere

SO/PHI - science

SO/PHI will provide unique science

- Provide B to EUV imager and spectrometer, all observing at high spatial resolution (up to 180 km): linkage science
- First decent view of magnetic and velocity field at poles
- Follow surface and subsurface evolution of solar features (e.g. active regions) without changing viewing angle
- Stereoscopic helioseismology to better probe the interior
- Stereoscopy of the photosphere

SO/PHI - high latitude science

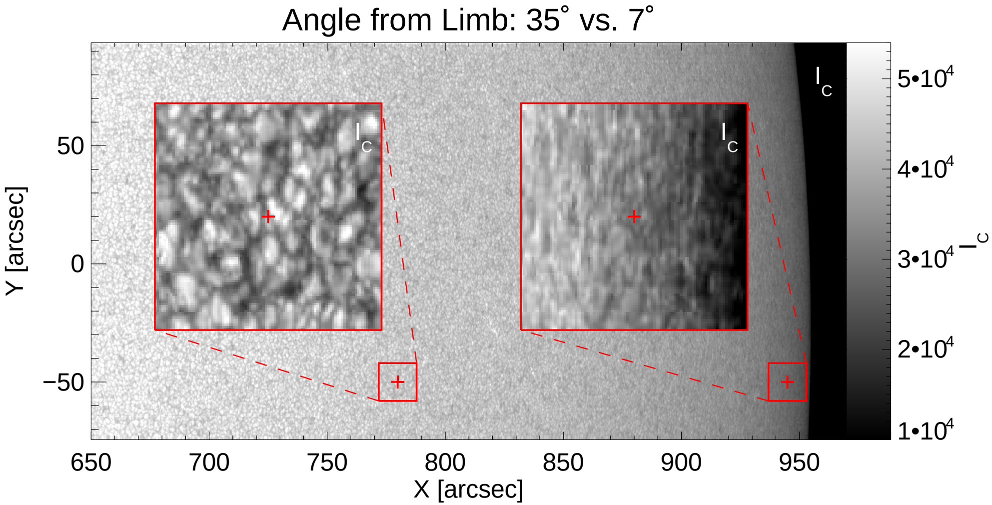

SO/PHI - basics

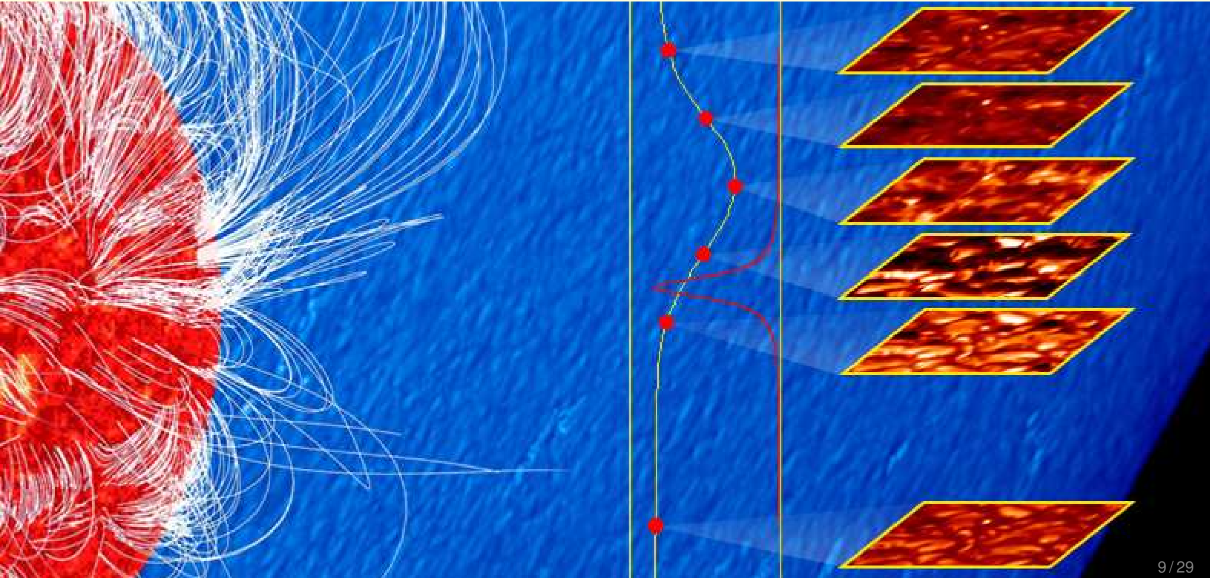

SO/PHI - basics

SO/PHI specs

- mass: 34 kg
- power: ≈31 W
- data rate: 20 kbps

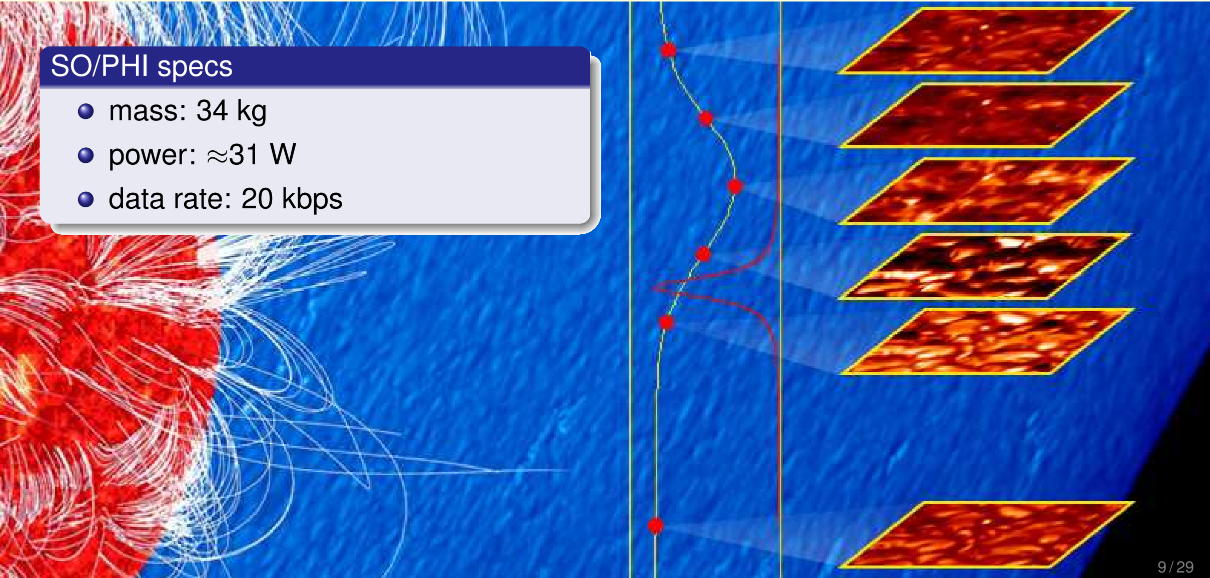

SO/PHI - basics

SO/PHI specs

- mass: 34 kg
- power: ≈31 W
- data rate: 20 kbps

SO/PHI measurement

- Doppler and Zeeman effects in Fe I 6173 Å
- 2D intensity maps at
  - 6 λ points within the line
  - *IQUV* at each λ point
- similar to Sunrise IMaX

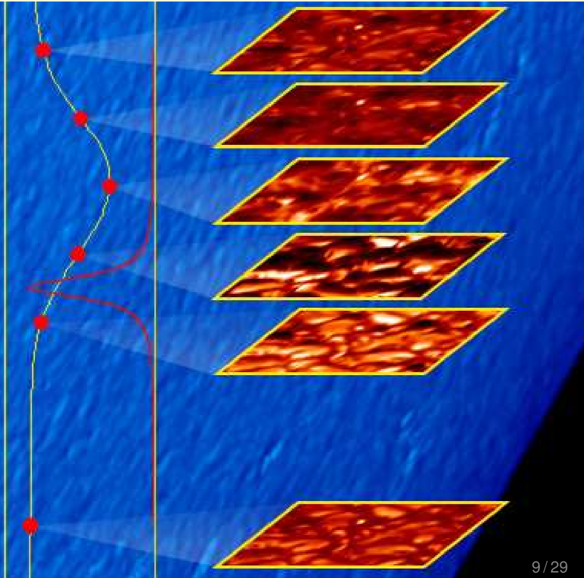

Polarimetric and Helioseismic Imager

SO/PHI instrument

- HRT: 14 cm reflector, 16.8 arcmin FOV
- FDT: 1.75 cm refractor, 2° FOV
- feed selection mech.
- Fabry-Pérot NB filter with $LiNbO_3$ etalon
- Polarisation modulation with LC variable retarders
- Single 2k × 2k APS

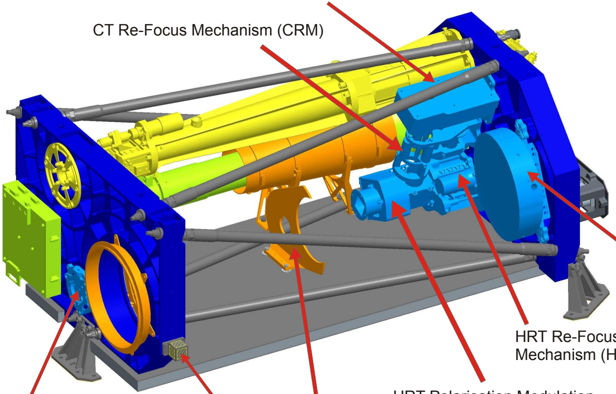

Polarimetric and Helioseismic Imager

SO/PHI instrument

- HRT: 14 cm reflector, 16.8 arcmin FOV
- FDT: 1.75 cm refractor, 2° FOV
- feed selection mech.
- Fabry-Pérot NB filter with $LiNbO_3$ etalon
- Polarisation modulation with LC variable retarders
- Single 2k × 2k APS

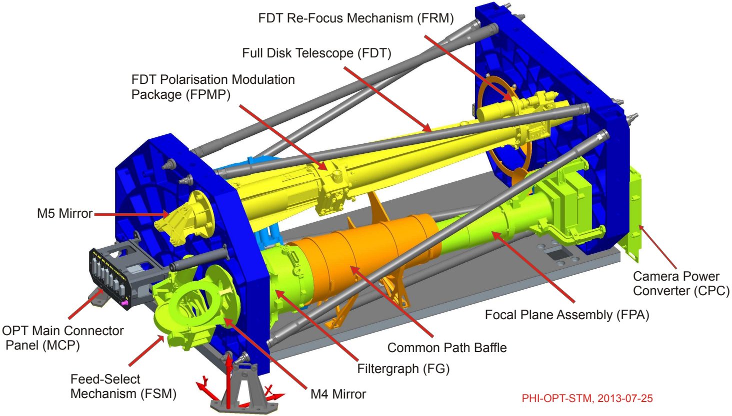

SO/PHI - technical challenges

SO/PHI challenges

- orbit (change of heat load):
  45 W (0.7 AU) – 290 W (0.28 AU) on entrance window
- heat (entrance window): radial temperature gradient
  $\longrightarrow$ optical performance
- image stabilization: single beam configuration (0.03” rms)
- data rate:
  - 2k $\times$ 2k, 12 bit, 6 WL-points, 4 Stokes, 1 min^{-1}, $>$200 GByte/day
  - available (20 kbps average): 216 Mbyte/day
  - $\rightarrow$ efficient data compression required:
    on-board data reduction & Milne-Eddington inversions ($\times$30–35)
  - $\rightarrow$ data selection (closest approach windows, ME parameter map selection)
  - $\rightarrow$ lossy compression
- power, radiation, . . .

SO/PHI - Magnetometry

On-board inversions

- near real-time inversions on VIRTEX-4 FPGA
- 9 free parameters per pixel: B, γ, ϕ, v_{LOS}, v_{dopp}, a_{damp}, η_0, S_0, S_1
- transmit only subset to ground (typical: I_C, B, γ, ϕ, v_{LOS})
- 4-5 bit per parameter
- compression ratio: $\times$30–35

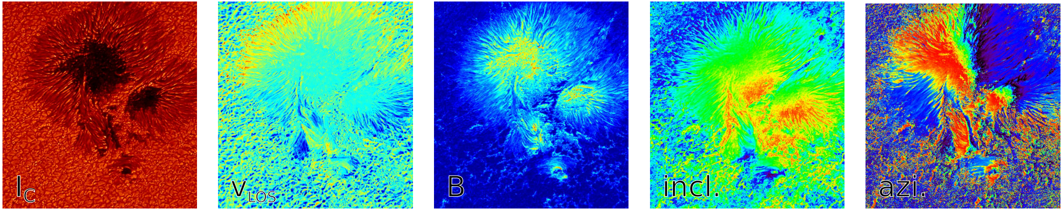

Ground-based magnetometry in 2020

Morning session

Thomas Rimmele, Dirk Soltau, Siraj Hasan

Existing Telescopes

- NST
- GREGOR
- SST
- ...

Future Telescopes

- ATST
- **EST**
- Indian NLST
- Chinese GST
- ...

Future Magnetometry

$\longrightarrow$ vector magnetic fields $<0\overset{''}{.}05$

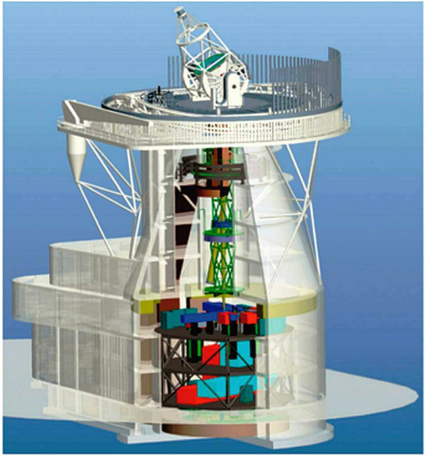

Advanced instrumentation

Instrumentation

- multi-slit instruments
- 2D spectropolarimeters (fiber optics, microlense arrays)

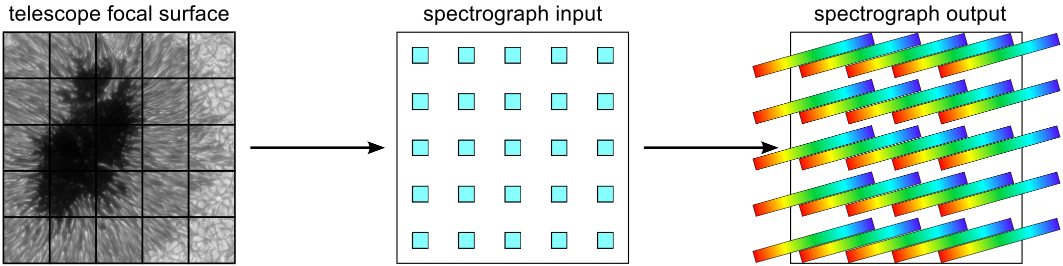

Advanced analysis

Analysis

- advances in data reduction (e.g. MOMFBD)
- spatially coupled inversions (van Noort 2012): (good knowledge of PSF required!)
- non-LTE inversions (de la Cruz Rodríguez et al. 2012)
- MHD-based inversions

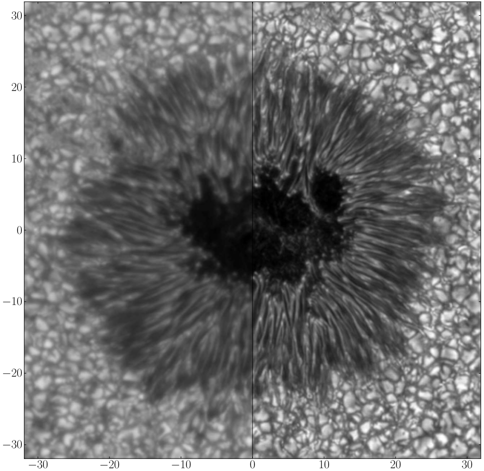

Advanced analysis

Analysis

- advances in data reduction (e.g. MOMFBD)
- spatially coupled inversions (van Noort 2012): (good knowledge of PSF required!)
- non-LTE inversions (de la Cruz Rodríguez et al. 2012)
- MHD-based inversions

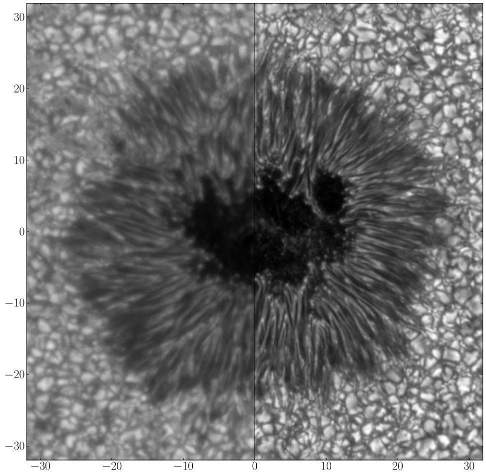

Advanced analysis

Analysis

- advances in data reduction (e.g. MOMFBD)
- spatially coupled inversions (van Noort 2012): (good knowledge of PSF required!)
- non-LTE inversions (de la Cruz Rodríguez et al. 2012)
- MHD-based inversions

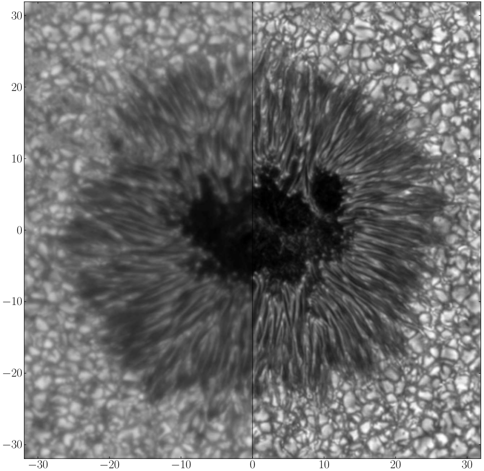

Advanced analysis

701

Analysis

- advances in data reduction (e.g. MOMFBD)
- spatially coupled inversions (van Noort 2012): (good knowledge of PSF required!)
- non-LTE inversions (de la Cruz Rodríguez et al. 2012)
- MHD-based inversions

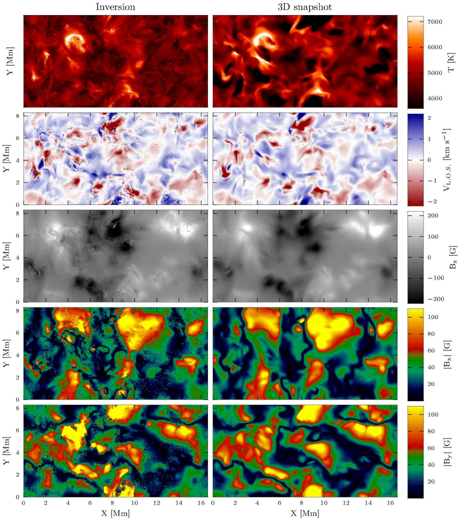

Stereoscopy with SO/PHI

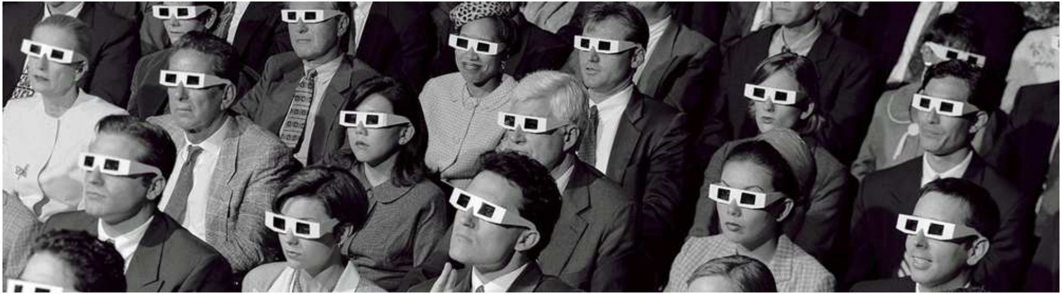

- Stereoscopic helioseismology
  Jesper Schou (16:00)
- 3D-velocity vectors
- Azimuth ambiguity
- Height information
- Scattering polarization
- Magnetic coupling

Full 3D-velocity vectors

LOS-velocities

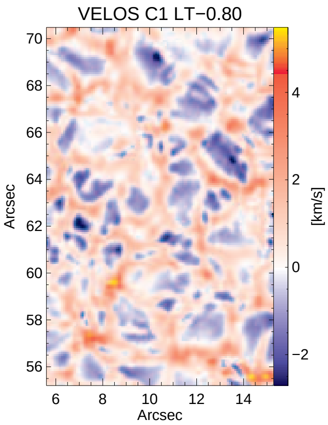

Obtaining 3D-velocities

Combining Doppler maps (LOS-comp.) with feature tracking (horiz. comp.)

Danger: gas motions $\neq$ motion of features

$\rightarrow$ 3D vector determination usually impossible

with SO/PHI + GB: stereoscopic feature tracking & stereoscopic Doppler measurements

Horizontal velocities

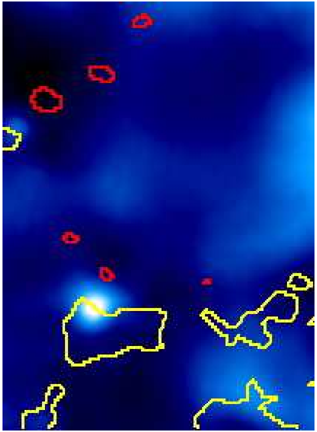

Jafarzadeh et al. (2013)

Full 3D-velocity vectors

LOS-velocities

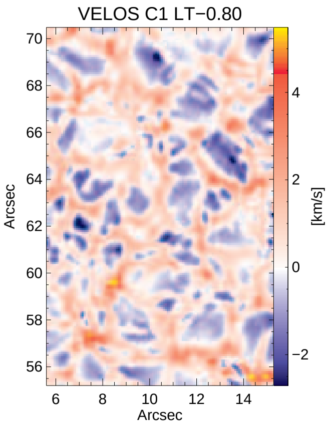

Convective motions

- determination of horizontal component possible
- granules, LBs, umbral dots, . . .

Penumbral fine structure

- direct measurement of the inclination of the Evershed flow
- understand mass balance & convective nature of filaments

Horizontal velocities

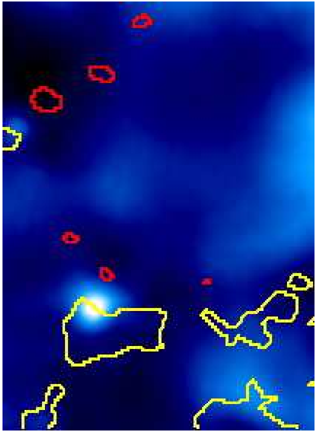

Jafarzadeh et al. (2013)

Azimuth ambiguity

Zeeman-polarimetry intrinsic problem: $2\chi \propto \tan Q/U$

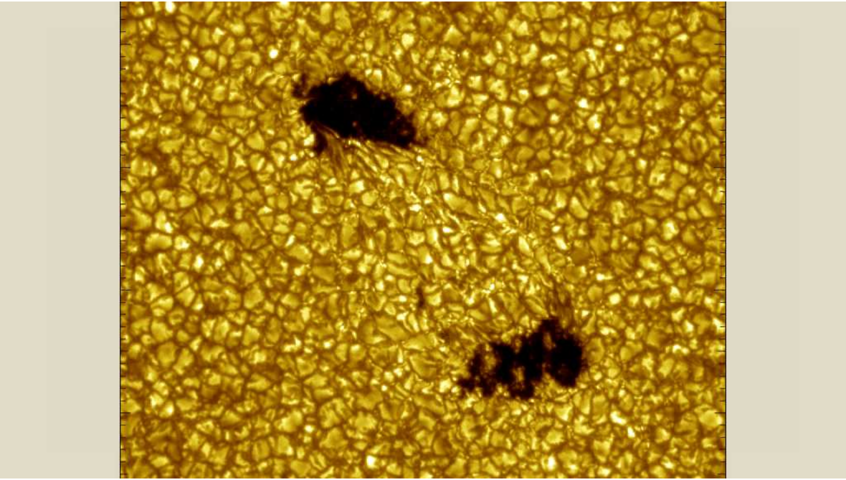

Azimuth ambiguity

Tools (Metcalf et al. 2006)

Method	Quantity minimized	Minimization scheme
Acute angle	$\lvert\theta_o - \theta_e\rvert$	Local
Large scale potential	$\lvert\theta_o - \theta_e\rvert$	Scale variation
USM	$\lvert\theta_o - \theta_e - \theta_{mp}\rvert$	Local
Magnetic pressure gradient	$\partial B^2/\partial z$	Local
Minimum structure	$\omega_s \partial B/\partial z + \omega_p \lvert J_{2_z}\rvert$	Local+smoothing
NPFC	$\lvert J_z\rvert$	Iterative
Pseudo-current	$d^2a\ J_z^2$	Conjugate gradient
UH iterative	$d^2a\ J_z^2$	Iterative
Minimum energy	$d^2a\ (\lvert J\rvert + \lvert\nabla \cdot B\rvert)^2$	Simulated annealing
AZAM	Angle between neighboring pixels	Interactive

Azimuth ambiguity

Tools (Metcalf et al. 2006)

Method	Quantity minimized	Minimization scheme
Acute angle	$\lvert\theta_o - \theta_e\rvert$	Local
Large scale potential	$\lvert\theta_o - \theta_e\rvert$	Scale variation
USM	$\lvert\theta_o - \theta_e - \theta_{\mathrm{mp}}\rvert$	Local
Magnetic pressure gradient	$\partial B^2/\partial z$	Local
Minimum structure	$\omega_s \partial B/\partial z + \omega_p \lvert J_{2_z}\rvert$	Local+smoothing
NPFC	$\lvert J_z\rvert$	Iterative
Pseudo-current	$d^2a\ J_z^2$	Conjugate gradient
UH iterative	$d^2a\ J_z^2$	Iterative
Minimum energy	$d^2a\ (\lvert J\rvert + \lvert\nabla \cdot B\rvert)^2$	Simulated annealing
AZAM	Angle between neighboring pixels	Interactive

Leka et al. (2009); Crouch (2013)

"No method ever produced a perfect solution to any of the cases tested when noise was present; no method ever perfectly resolved the ambiguity in areas which were not spatially resolved."

Azimuth ambiguity

Unique solution: observation under different viewing angle

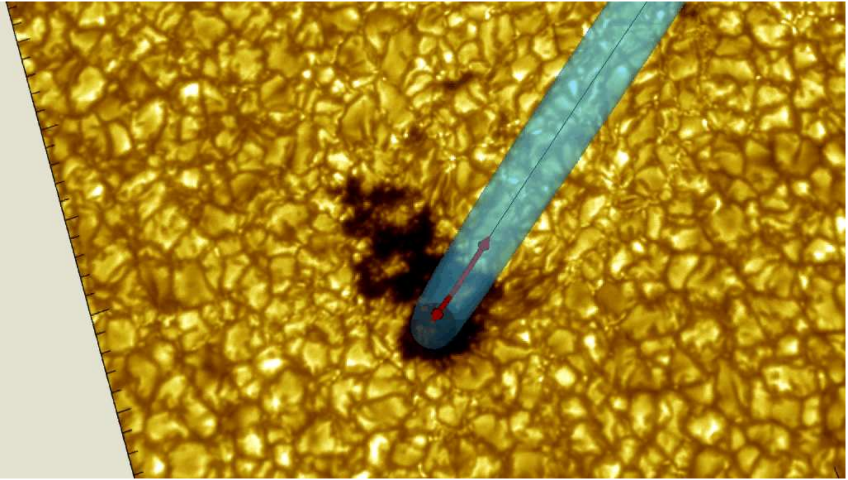

Scattering polarization

Hanle effect

e.g. Sr I 4607 Å

- strongest scattering polarization signals close to limb, where Zeeman signals are weakest
- SO/PHI offers independent “disk-center” measurements
- help to disentangle
  - collisional vs. Hanle depolarization
  - turbulent / non turbulent fields

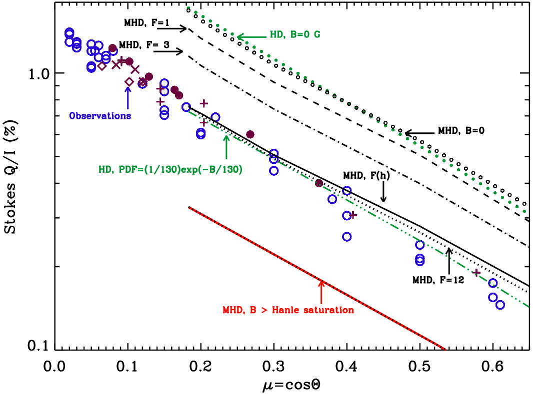

Shchukina & Trujillo Bueno (2013);
Trujillo Bueno et al. (2004)

Height information - Wilson depression

Height estimate: force balance

Mathew et al. (2004)

$$
\begin{aligned}
P_0(z) \; = \; & \\
& P_G(r,z) \\
& + B_z^2(r,z)/8\pi \\
& + F_c(r,z)/8\pi
\end{aligned}
$$

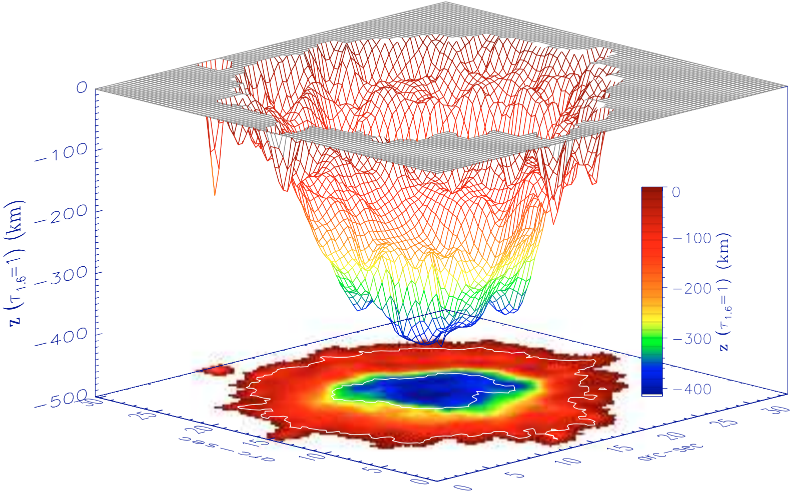

Height information - Light bridge ”mountains”

Lites et al. (2004): “triangulation” 300±50 km

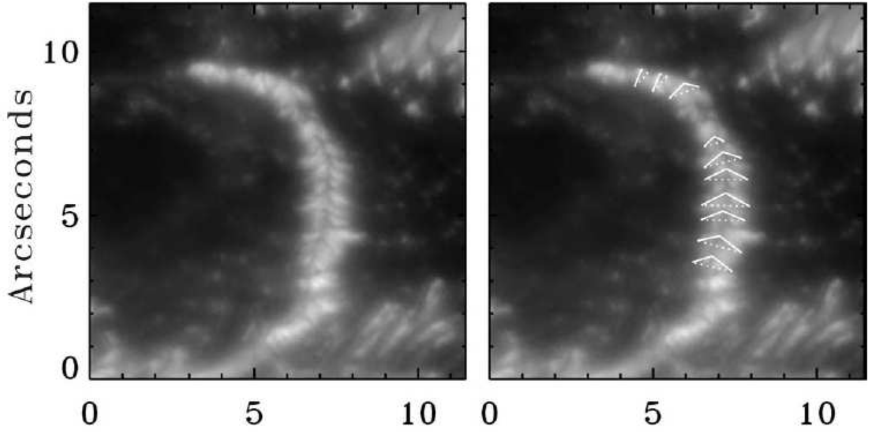

“Regular” stereoscopy

STEREO

- proven concept for CMEs, loops, prominences
- e.g. Wiegelmann et al. (2009); Mierla et al. (2013); de Patoul et al. (2013); Feng et al. (2013)

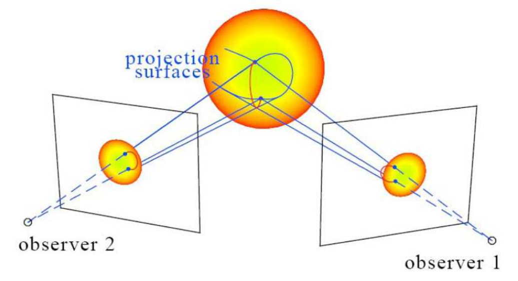

Requirements for applications to photosphere

- extremely accurate co-alignment with ground-based imaging instruments
- co-temporal measurements

“Inversion” stereoscopy

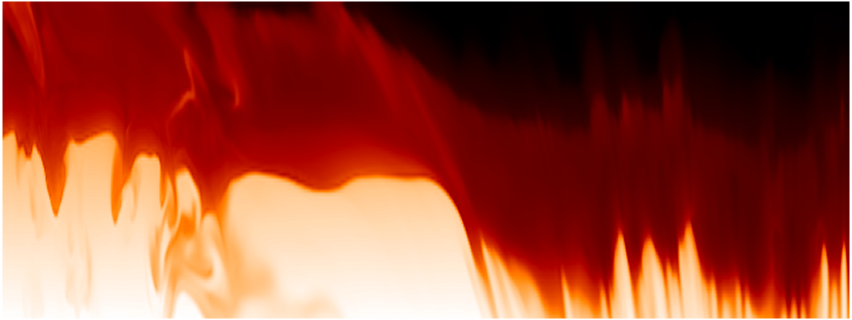

Vertical temperature cut through MURaM-sunspot (Rempel et al. 2009)

“Inversion” stereoscopy

GB measurement

- highest spatial resolution (≈50 km)
- many spectral lines
- good log τ coverage

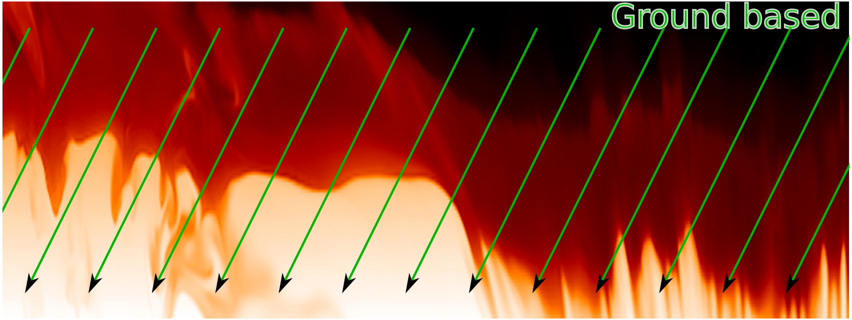

Vertical temperature cut through MURaM-sunspot (Rempel et al. 2009)

"Inversion" stereoscopy

GB measurement

- highest spatial resolution ($\approx$50 km)
- many spectral lines
- good log τ coverage

SO/PHI measurement

- $\approx$180 km resolution
- Fe I 6173 Å line
- ME averaged parameters

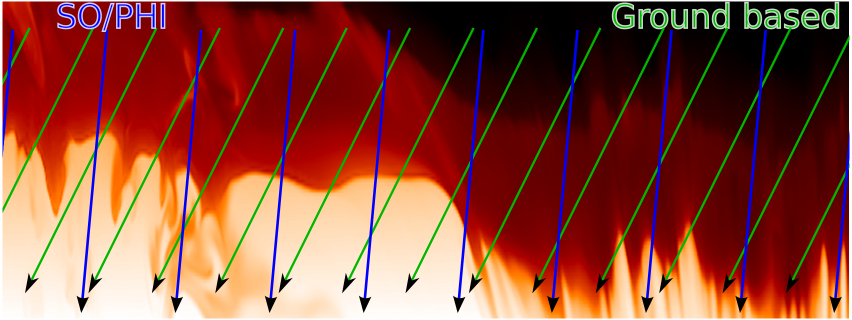

Vertical temperature cut through MURaM-sunspot (Rempel et al. 2009)

“Inversion” stereoscopy

GB measurement

- highest spatial resolution ($\approx$50 km)
- many spectral lines
- good log τ coverage

SO/PHI measurement

- $\approx$180 km resolution
- Fe I 6173 Å line
- ME averaged parameters

"Inversion" stereoscopy

GB measurement

- highest spatial resolution (≈50 km)
- many spectral lines
- good $\log\tau$ coverage

SO/PHI measurement

- ≈180 km resolution
- Fe I 6173 Å line
- ME averaged parameters

Spatially coupled inversion

1. solve RTE for GB data in 2D ($\log\tau$)
2. convert $\log\tau \rightarrow z$ using, e.g., force balance
3. tilt this cube to SO/PHI viewing angle
4. simulate ME measurement from this cube
5. iteratively adjust height for every pixel until best match with SO/PHI ME measurements

“Inversion” stereoscopy

GB measurement

- highest spatial resolution (≈50 km)
- many spectral lines
- good log τ coverage

SO/PHI measurement

- ≈180 km resolution
- Fe I 6173 Å line
- ME averaged parameters

Spatially coupled inversion

1. solve RTE for GB data in 2D (log τ)
2. convert log $\tau \rightarrow z$ using, e.g., force balance
3. tilt this cube to SO/PHI viewing angle
4. simulate ME measurement from this cube
5. iteratively adjust height for every pixel until best match with SO/PHI ME measurements

"Inversion" stereoscopy

GB measurement

- highest spatial resolution (≈50 km)
- many spectral lines
- good log τ coverage

SO/PHI measurement

- ≈180 km resolution
- Fe I 6173 Å line
- ME averaged parameters

Spatially coupled inversion

1. solve RTE for GB data in 2D (log τ)
2. convert log τ $\rightarrow$ z using, e.g., force balance
3. tilt this cube to SO/PHI viewing angle
4. simulate ME measurement from this cube
5. iteratively adjust height for every pixel until best match with SO/PHI ME measurements

"Inversion" stereoscopy

GB measurement

- highest spatial resolution (≈50 km)
- many spectral lines
- good $\log\tau$ coverage

SO/PHI measurement

- ≈180 km resolution
- Fe I 6173 Å line
- ME averaged parameters

Spatially coupled inversion

1. solve RTE for GB data in 2D ($\log\tau$)
2. convert $\log\tau \rightarrow z$ using, e.g., force balance
3. tilt this cube to SO/PHI viewing angle
4. simulate ME measurement from this cube
5. iteratively adjust height for every pixel until best match with SO/PHI ME measurements

"Inversion" stereoscopy

GB measurement

- highest spatial resolution (≈50 km)
- many spectral lines
- good $\log\tau$ coverage

SO/PHI measurement

- ≈180 km resolution
- Fe I 6173 Å line
- ME averaged parameters

Spatially coupled inversion

1. solve RTE for GB data in 2D ($\log\tau$)
2. convert $\log\tau \rightarrow z$ using, e.g., force balance
3. tilt this cube to SO/PHI viewing angle
4. simulate ME measurement from this cube
5. iteratively adjust height for every pixel until best match with SO/PHI ME measurements

“Inversion” stereoscopy

GB measurement

- highest spatial resolution (≈50 km)
- many spectral lines
- good log τ coverage

SO/PHI measurement

- ≈180 km resolution
- Fe I 6173 Å line
- ME averaged parameters

Spatially coupled inversion

1. solve RTE for GB data in 2D (log τ)
2. convert log $\tau \rightarrow z$ using, e.g., force balance
3. tilt this cube to SO/PHI viewing angle
4. simulate ME measurement from this cube
5. iteratively adjust height for every pixel until best match with SO/PHI ME measurements

Height information - application

Mass balance in penumbral filaments

discrepancies in literature:

- 2–3$\times$ excess in downward flux (e.g. Westendorp Plaza et al. 1997; Tiwari et al. 2013)
- 5$\times$ excess in upflow (Puschmann et al. 2010)

using height info & 3D-velocities:

- avoid corrugation of iso-τ layers
- full characterization of Evershed flow
- true mass balance can be determined
- applicable to, e.g., umbral dots, LBs

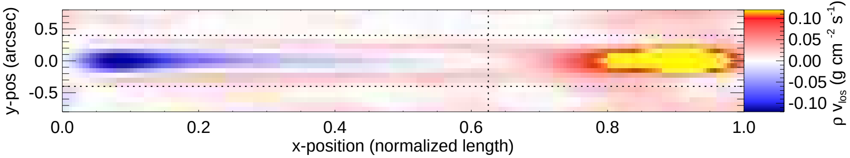

Mass flux in a “standard filament” at $\log \tau = 0$ (Tiwari et al. 2013)

Magnetic coupling

Valuable input for extrapolations

- + stereoscopic observations of coronal loops (SDO & SolO)
- + stereoscopic observations of photospheric field (GB & SO/PHI)
- + 180° ambiguity free

→ perfect prerequisites for extrapolations

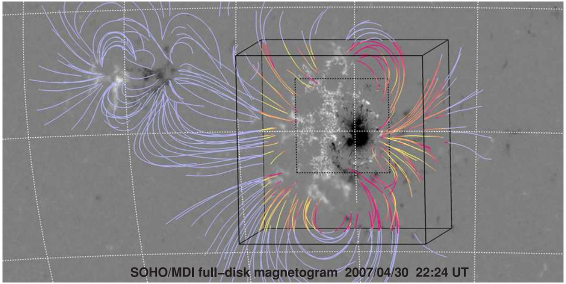

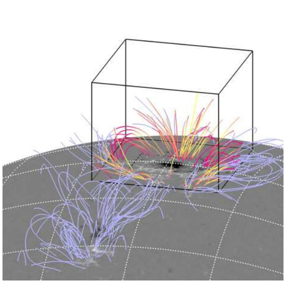

De Rosa et al. (2009)

Summary & Conclusion

Summary

- Solar Orbiter's strength is the simultaneous, multi-instrument measurements of solar phenomena
- Magnetometry with SO/PHI: limitations due to size, power, data rate
- Hi-res ground-based observations can ideally compensate these limitations
- enhances scienctific output for both, Solar Orbiter and ground-based observatories

Summary & Conclusion

Summary

- Solar Orbiter's strength is the simultaneous, multi-instrument measurements of solar phenomena
- Magnetometry with SO/PHI: limitations due to size, power, data rate
- Hi-res ground-based observations can ideally compensate these limitations
- enhances scienctific output for both, Solar Orbiter and ground-based observatories

Requirement:

Good coordination between GB facilities, earth orbiting observatories and SolO science operation group, especially during CA and times of special orbital configuration.

Bilbiography

Crouch, A. D. 2013, Sol. Phys., 282, 107

de la Cruz Rodríguez, J., Socas-Navarro, H., Carlsson, M., & Leenaarts, J. 2012, A&A, 543, A34

de Patoul, J., Inhester, B., Feng, L., & Wiegelmann, T. 2013, Sol. Phys., 283, 207

De Rosa, M. L., Schrijver, C. J., Barnes, G., et al. 2009, ApJ, 696, 1780

Feng, L., Wiegelmann, T., Su, Y., et al. 2013, ApJ, 765, 37

Jafarzadeh, S., Solanki, S. K., Feller, A., et al. 2013, A&A, 549, A116

Leka, K. D., Barnes, G., Crouch, A. D., et al. 2009, Sol. Phys., 260, 83

Lites, B. W., Scharmer, G. B., Berger, T. E., & Title, A. M. 2004, Sol. Phys., 221, 65

Mathew, S. K., Solanki, S. K., Lagg, A., et al. 2004, A&A, 422, 693

Metcalf, T. R., Leka, K. D., Barnes, G., et al. 2006, Sol. Phys., 237, 267

Mierla, M., Seaton, D. B., Berghmans, D., et al. 2013, Sol. Phys., 286, 241

Puschmann, K. G., Ruiz Cobo, B., & Martínez Pillet, V. 2010, ApJ, 720, 1417

Rempel, M., Schüssler, M., Cameron, R. H., & Knölker, M. 2009, Science, 325, 171

Shchukina, N. G. & Trujillo Bueno, J. 2013, in IAU Symposium, Vol. 294, IAU Symposium, ed. A. G. Kosovichev, E. de Gouveia Dal Pino, & Y. Yan, 107–118

Tiwari, S. K., van Noort, M., Lagg, A., & Solanki, S. K. 2013, ArXiv e-prints

Trujillo Bueno, J., Shchukina, N., & Asensio Ramos, A. 2004, Nature, 430, 326

van Noort, M. 2012, A&A, 548, A5

Westendorp Plaza, C., del Toro Iniesta, J. C., Ruiz Cobo, B., et al. 1997, Nature, 389, 47

Wiegelmann, T., Inhester, B., & Feng, L. 2009, Annales Geophysicae, 27, 2925